GFZ
Helmholtz-Zentrum
POTSDAM

Originally published as:

Bonaccorso, A., Aoki, Y., Rivalta, E. (2017): Dike propagation energy balance from deformation modeling and seismic release. - *Geophysical Research Letters*, *44*, 11, pp. 5486—5494.

DOI: http://doi.org/10.1002/2017GL074008

AGU PUBLICATIONS

Geophysical Research Letters

RESEARCH LETTER
10.1002/2017GL074008

Key Points:
- The study investigated the relationship between the deformation induced by dike propagation leading to eruptions and the released seismic energy
- We individuated a simple equation that can be used as a proxy of the expected mechanical energy released by a propagating dike that is related to its average thickness
- We obtained an empirical law that quantifies the seismic moment released by a dike intrusion, thus providing a tool to control the energy status during its propagation

Correspondence to:
A. Bonaccorso,
alessandro.bonaccorso@ingv.it

Citation:
Bonaccorso, A., Y. Aoki, and E. Rivalta (2017), Dike propagation energy balance from deformation modeling and seismic release, *Geophys. Res. Lett.*, *44*, 5486–5494, doi:10.1002/2017GL074008.

Received 24 JAN 2017
Accepted 3 MAY 2017
Accepted article online 8 MAY 2017
Published online 14 JUN 2017

©2017. American Geophysical Union. All Rights Reserved.

Dike propagation energy balance from deformation modeling and seismic release

Alessandro Bonaccorso[1], Yosuke Aoki[2], and Eleonora Rivalta[3]

[1]Istituto Nazionale di Geofisica e Vulcanologia, Catania, Italy, [2]Earthquake Research Institute, University of Tokyo, Tokyo, Japan, [3]Helmholtz-Zentrum Potsdam-Deutsches GeoForschungsZentrum GFZ, Potsdam, Germany

Abstract Magma is transported in the crust mainly by dike intrusions. In volcanic areas, dikes can ascend toward the free surface and also move by lateral propagation, eventually feeding flank eruptions. Understanding dike mechanics is a key to forecasting the expected propagation and associated hazard. Several studies have been conducted on dike mechanisms and propagation; however, a less in-depth investigated aspect is the relation between measured dike-induced deformation and the seismicity released during its propagation. We individuated a simple x that can be used as a proxy of the expected mechanical energy released by a propagating dike and is related to its average thickness. For several intrusions around the world (Afar, Japan, and Mount Etna), we correlate such mechanical energy to the seismic moment released by the induced earthquakes. We obtain an empirical law that quantifies the expected seismic energy released before arrest. The proposed approach may be helpful to predict the total seismic moment that will be released by an intrusion and thus to control the energy status during its propagation and the time of dike arrest.

Plain Language Summary Dike propagation is a dominant mechanism for magma ascent, transport, and eruptions. Besides being an intriguing physical process, it has critical hazard implications. After the magma intrusion starts, it is difficult to predict when and where a specific horizontal dike is going to halt and what its final length will be. In our study, we singled an equation that can be used as a proxy of the expected mechanical energy to be released by the opening dike. We related this expected energy to the seismic moment of several eruptive intrusions around the world (Afar region, Japanese volcanoes, and Mount Etna). The proposed novel approach is helpful to estimate the total seismic moment to be released, therefore allowing potentially predicting when the dike will end its propagation. The approach helps answer one of the fundamental questions raised by civil protection authorities, namely, "how long will the eruptive fissure propagate?"

1. Introduction

Dike propagation is a dominant mechanism for magma ascent, transport, and emplacement in the crust. Flank eruptions on volcanoes are often fed by dikes that move for several kilometers, driving magma, previously accumulated in a reservoir. The greatest hazards on a global scale are for large fissure eruptions that are mostly fed in vertical flow from deep-seated reservoirs [*Gudmundsson*, 2016]. However, also, smaller eruptions are potentially damaging to infrastructures depending on the dike propagation. In general, hazards associated with lateral dike propagation are greater for longer dikes that can reach the outer flanks of a volcano: the longer the propagation, the more dangerous it becomes because the intrusion may approach towns and man-made infrastructures, often located on the lower volcano flanks. As examples, the 1669 eruption of Etna volcano (Sicily, Italy) destroyed the town of Catania (located close to the sea, 30 km from the summit) due to an eruptive fissure that propagated 16 km toward the town and then fed an eruptive vent in the low flank. An eruption similar to the one occurring in 1669 would result in damage amounting to about 7 billion Euros [*Del Negro et al.,* 2016].

In Japan, Sakurajima volcano has erupted several times through radial dikes, as, for instance, in 1476, 1779, and 1914. The 1914 eruption produced lava that flowed into the Seto strait connecting the island of Sakurajima with the Oosumi peninsula. Recently, in August 2015, ground deformation indicated propagation of an intrusion that fortunately stopped and did not evolve into an eruption [*Hotta et al.,* 2016; *Morishita et al.,* 2016]. Offshore the Izu Peninsula, ~100 km southwest of Tokyo, seismic swarms recurred approximately once a year in the 1980s and 1990s. Geodetic data show that the seismic swarms are due to horizontal dike

propagation [*Okada and Yamamoto*, 1991; *Aoki et al.,* 1999; *Morita et al.,* 2006]. Most of the dike intrusions were arrested before reaching the surface, but the 1989 dike intrusion resulted in a submarine eruption [*Okada and Yamamoto*, 1991].

Besides Etna and the above mentioned Japanese volcanoes, this kind of process has been observed at several basaltic volcanoes around the world such as at Kilauea, Hawaii [e.g., *Rubin*, 1990], Piton de la Fournaise, Reunion Island [e.g., *Peltier et al.,* 2005], and rift systems such as those in Iceland and Afar (Ethiopia) [e.g., *Gudmundsson*, 1983, 2011; *Rubin and Pollard*, 1988; *Grandin et al.,* 2011].

Understanding the mechanisms controlling dike propagation has always been a central issue in volcano physics, and a related issue of great interest is dike arrest. In most cases horizontally or vertically propagating dikes stop before intersecting the surface [e.g., *Gudmundsson et al.,* 1999; *Gudmundsson*, 2003]. Dike arrest may occur because a dike loses buoyancy or driving pressure [e.g., *Rivalta*, 2010; *Taisne et al.,* 2011], or due to magma solidification [e.g., *Lister and Kerr*, 1991], or again to a structural barrier [e.g., *Gudmundsson*, 2011; *Geshi et al.,* 2012], or even to stress perturbation by a big earthquake, or creeping on large faults [*Maccaferri et al*., 2015, *Xu et al.,* 2016]. Besides the numerical approach [e.g., *Pollard and Muller*, 1976; *Rubin and Pollard*, 1987], dikes have been studied following different approaches including field mapping [e.g., *Delaney and Gartner*, 1997; *Reches and Fink*, 1988; *Gudmundsson*, 2002; *Poland et al.,* 2008, *Kavanagh and Sparks*, 2011] and analogue lab experiments [e.g., *McLeod and Tait*, 1999; *Takada*, 1990; *Menand and Tait*, 2002; *Taisne and Tait*, 2009; *Traversa et al.,* 2010]. Review articles on magma-driven fracture modeling include those by *Pollard* [1987] for the solid mechanics, *Lister and Kerr* [1991] for coupling the fluid flow and elastic deformation, *Rubin* [1995] with considerations on dike initiation and propagation, and *Rivalta et al.* [2015] for basic concepts and mechanical models.

Once the potential causes of dike arrest have been identified, mechanical modeling may be used to assess their relative contribution [e.g., *Gudmundsson*, 2006, 2011; *Maccaferri et al*., 2015], but such a method requires constraints on many parameters and is unsuitable for real-time forecasting. A general propagation criterion can be defined as the stress intensity factor reaching a critical value $K = K_c$, where K_c, the fracture toughness, measures the resistance of the rock to crack propagation [i.e., *Rubin*, 1993]. Field observations show much higher K_c values (usually about $10–10^2$ MPa $m^{0.5}$) than expected from experimental lab measurements (typically in the order of 1 MPa $m^{0.5}$). *Gudmundsson* [2009] proposed that composite volcanic edifices with multiple layers of different strength may result in higher average fracture toughness. *Rubin et al.* [1998] noted that the seismicity induced by dikes constitutes a sink of energy; it provides evidence of a release of fracture energy beyond what is needed to elongate the intrusion. *Morita et al.* [2006], for example, inferred the geometry of the 1998 dike intrusion at Izu Peninsula by deformation and seismic data. They concluded that K_c is not representable by a constant value during dike growth. Lab analogue experiments of fluid injection [i.e., *Menand and Tait*, 2002] also suggested that the resistance to propagation did not remain constant but increased as the fissure propagated. A scale relation for K_c is an open question in literature, and a better definition would be important to reconcile the different values obtained. The dissipation of energy will be mirrored into an effective (also called apparent) value of K_c, scaling with the dimension of the dike [*Rivalta et al.,* 2015].

Identifying observables of the energy released during diking and clarifying their mutual relationship may help in designing a simpler forecasting method. In recent decades, deformation and seismic changes associated with several intrusions have provided the opportunity to estimate the approximate shape and geometry of the intrusions and infer the released seismic energy, respectively. The goal of our study is to analyze simultaneously the modeled dike growth and the seismic energy released during intrusions at different volcanoes. The aim is to constrain general features of dike propagation and better understand the conditions leading to dike arrest.

Starting from the basic concepts of magma-driven fractures and linear elastic theory, we derive an equation that mirrors the expected available mechanical energy U_E to be released depending on the opening of the dike (i.e., its thickness). We consider several eruptions (Etna, Japan, and Afar) with dike parameters inferred by modeled deformation and recorded seismicity. We relate U_E to the recorded total seismic moment and use this to estimate the seismic energy that will be released after the dike has opened and starts to propagate. We discuss how this approach may help evaluating a priori how long an eruptive fracture might be.

2. A Novel Approach to Estimate Dike Energy From Geophysical Measurements

Our investigation deals with magma-driven fractures that transport magma both vertically and horizontally without significant cooling and solidification before arrest. Magma intrusion is a complicated phenomenon with several processes storing and dissipating energy, such as the following: (i) elastic energy is stored in the surrounding rock with the opening of the dike walls; (ii) rock fracturing or slip on preexisting fractures dissipates energy around the tip and in the walls of the dike. Previous studies [i.e., *Lister and Kerr,* 1991] reckon this contribution as insignificant since it involves only a small part of the fracture (the tip), but this is debated [*Rivalta et al.,* 2015]; (iii) viscous magma flow within the dike also dissipates energy. Other processes provide energy to the system and contribute driving the dike, including the following: (i) buoyancy forces, due to the density difference between the magma and the host rock (this may often be neglected for horizontal dikes); (ii) compression caused by gradients of topographic loads or tectonic stress gradients; (iii) contribution of magma reservoir overpressure; and (iv) contribution of magma compression.

The driving pressure, P_d, superposition of several such contributions, is defined as the difference between the magma pressure and the total horizontal stress perpendicular to the plane of the dike. The thickness to length ratio of a dike is related to the pressure available to open the dike walls and the resistance of the host rock to opening. Following the linear elastic theory in literature, the equation mainly used [*Pollard*, 1987; *Rubin*, 1995] is

$$P_d = t/2a \times \mu/(1-\nu) \tag{1}$$

where $2a$ is the length of the stationary fluid-filled dike, t the dike thickness, μ the medium rigidity, and ν the Poisson coefficient, and the ratio $\mu/(1-\nu)$ is known as the host-rock stiffness.

Irwin [1957] reconciled the K_c criterion with that based on Griffith's global energy balance [*Griffith*, 1921], showing that a critical value K_c criterion is equivalent to one requiring that the energy release rate reaches a critical value $G = G_c$, where $G = -\partial U_E/\partial a$, with U_E the elastic strain energy of the brittle elastic solid that decreases by increasing the crack length a. For a blade-like dike of length $2a$ in plane strain, *Pollard* [1987] showed that the change in elastic strain energy of the host rock caused by dike dilatation is

$$U_E = \pi a^2 {P_d}^2 [(1-\nu)/2\mu] \tag{2}$$

This can be considered a more general relation since U_E may include energy dissipated through other mechanisms besides the one spent in the tip opening [*Pollard*, 1987]. The unit is energy per unit length of the dike in the direction perpendicular to the propagation and the opening.

By combining equations (1) and (2), we obtain the available mechanical elastic strain energy U_E as a function of dike thickness:

$$U_E = \pi/4 \cdot \mu/(1-\nu) \cdot t^2 \tag{3}$$

This equation is useful because it relates the available elastic strain energy to just one dynamic parameter of the dike, its thickness. Note that we consider dikes that have propagated for a considerable distance (greater than the chamber radius) away from the chamber, so that we disregard any influence of magma chamber pressurization on the strain. Tectonic contributions to strain are incorporated by defining the driving pressure as $P - S$, difference between magma pressure, P, and regional compressive stress, S.

Numerical models and laboratory experiment studies show that a dike propagating in a homogeneously stressed medium fed by constant influx of magma is formed by an inflated propagating "head" or "nose" region, whose shape does not change much during propagation, followed by a constant-thickness tail [e.g., *Heimpel and Olson*, 1994, *Taisne et al.,* 2011]. Analogue experiments have been more focused on propagation effects/characteristics; however, in recent studies [e.g., *Acocella et al.,* 2013; *Daniels and Menand*, 2015] there are confirmations of the near-uniform thickness of the reproduced dikes. Although dikes do show local variations in thickness when crosscutting layers with different elastic parameters (e.g., *Geshi et al.* [2010] or *Bonafede and Rivalta* [1999], for an analytical model), we disregard this aspect here for the sake of generality. In real cases, the presence of layered rocks and strong contrast in rigidity between different layers could produce dike arrest [e.g., *Geshi et al.,* 2012; *Gudmundsson*, 2002]. On the scale of dike length, small-scale complexities may be neglected and observations indicate that near-uniform thickness can be assumed to explain large-scale deformation such as recorded by geophysical monitoring networks. In considering the near

Table 1. Parameters of Different Eruptive Dike Eruptions Modeled From Ground Deformation and Associated Total Seismic Moment M_o Released During the Dike Intrusion

Location	Dike Type	Length (m)	Width (m)	Thickness (m)	Total Seismic Moment M_o (Nm)	Reference
East Izu 1989a	vertical	1,500	6,000	0.25	8.93E+12	*Okada and Yamamoto* [1991]
East Izu 1989b	vertical	3,000	6,000	1.45	6.09E+17	*Okada and Yamamoto* [1991]
East Izu 1997	vertical	8,000	10,000	0.2	1.36E+18	*Aoki et al.* [1999]
East. Izu 1998	vertical	4,000	3,000	2.5	1.04E+18	*Morita et al.* [2006, Model 1]
East Izu 1998	vertical	3,000	2,000	5	1.04E+18	*Morita et al.* [2006, Model 2]
East Izu 1998	vertical	2,000	1,000	15	1.04E+18	*Morita et al.* [2006, Model 3]
Izu Islands 2000	horizontal	21,900	1,000	28.8	3.65E+19	*Ozawa et al.* [2004]
Izu Islands 2000	horizontal	18,000	19,300	3.1	3.63E+19	*Ito and Yoshioka* [2002]
Izu Islands 2000	horizontal	20,000	10000	6	3.64E+19	*Yamaoka et al.* [2005, Model 2]
Izu Islands 2000	horizontal	20,000	10,000	10		*Yamaoka et al.* [2005, Model 3]
Etna 1981	p1-vertical	3,000	1,400	5.2		*Bonaccorso* [1999]
Etna 1981	p2-horizontal	6,600	400	1.1		*Bonaccorso* [1999]
Etna 1983	horizontal	3,500	1,000	1.5		*Murray and Pullen* [1984]
Etna 1989	horizontal	7,000	1,300	1		*Bonaccorso and Davis* [1993]
Etna 1991	horizontal	3,600	800	2.8		*Bonaccorso* [1996]
Etna 2001	vertical	2,200	2,300	3.5	3.25E+16	*Bonaccorso et al.* [2002][a]
Etna 2002	vertical	3,100	1,000	1	4.2E+14	*Aloisi et al.* [2006][a]
Etna 2002	horizontal	6,400	2,250	3.35	1.9E+16	mean value from *Aloisi et al.* [2006][a]
Etna 2008	near horizontal	2,500	2,000	2	6.8E+15	*Napoli et al.* [2008][a]
			Afar 2005–2009			
d0	horizontal	5,200	4996	4.6	3.40E+18	*Grandin et al.* [2010, 2011]
d1	horizontal	14,000	8493	1.1	6.10E+16	*Grandin et al.* [2010, 2011]
d2	horizontal	10,000	5655	0.8	3.80E+14	*Grandin et al.* [2010, 2011]
d3	horizontal	13,000	7569	0.5		*Grandin et al.* [2010, 2011]
d4	horizontal	12,000	4158	0.9		*Grandin et al.* [2010, 2011]
d5	horizontal	14,000	5179	0.5		*Grandin et al.* [2010, 2011]
d6	horizontal	12,000	4142	1.1		*Grandin et al.* [2010, 2011]
d7	horizontal	23,000	10561	0.8	3.10E+16	*Grandin et al.* [2010, 2011]
d8	horizontal	27,000	5967	0.6		*Grandin et al.* [2010, 2011]
d9	horizontal	19,000	3905	0.6	3.90E+14	*Grandin et al.* [2010, 2011]
d10	horizontal	17,000	8235	1.4	2.80E+16	*Grandin et al.* [2010, 2011]
d11	horizontal	12,000	6958	0.9	7.30E+14	*Grandin et al.* [2010, 2011]
d12	horizontal	12,000	3883	0.9		*Grandin et al.* [2010, 2011]

[a]Seismic moment calculated from magnitude catalogues at www.ct.ingv.it [*Alparone et al.,* 2015] applying the relation from *Giampiccolo et al.* [2007].

constant thickness as a valid approximation, encouraging support comes from the exposed dikes, which represent a real picture of the intruding process below the free surface. At Etna, along the walls of the Valle del Bove depression the majority of measurements of hundreds of exposed dikes, whose vertical sections are visible even for several hundreds of meters, reveal near-uniform thickness [*Ferrari et al.,* 1991]. Exposed feeder dikes ($>$ 100 m long) in the caldera wall of Miyakejima volcano show an essentially constant thickness, except for the uppermost shallow 20–40 m due to the free surface effects [*Geshi et al.,* 2010; *Geshi and Oikawa*, 2014]. Many deformation studies in different volcanoes around the world match the data by using uniform thickness tensile dislocation, then supporting the idea that a mean constant thickness is representative of the intrusion. Dynamic inversions of crustal deformation data are also consistent with approximately constant-thickness propagation [e.g., *Segall et al.,* 2001, *Ozawa et al.,* 2004; *Morita et al.,* 2006, *Aloisi et al.,* 2006; *Ji et al.,* 2013]. Dynamic inversion of crustal deformation data from the exceptionally well-constrained 2014 intrusion at Bardarbunga-Holuhraun (Iceland) [*Sigmundsson et al.,* 2015] shows that the dike, once the propagating nose had passed, maintained an approximately constant thickness of 2–3 m with a larger opening (4–5 m) only in the terminal and shallower part of the intrusion [*Sigmundsson et al.,* 2015, Figure 3a].

Certainly, a crack model where the opening scales with length is not consistent with observations of propagating dikes. Obviously, in the real cases of heterogeneous medium many intrusions are not uniform in thickness and their surface opening-displacement can show variations. However, as an approximation, the

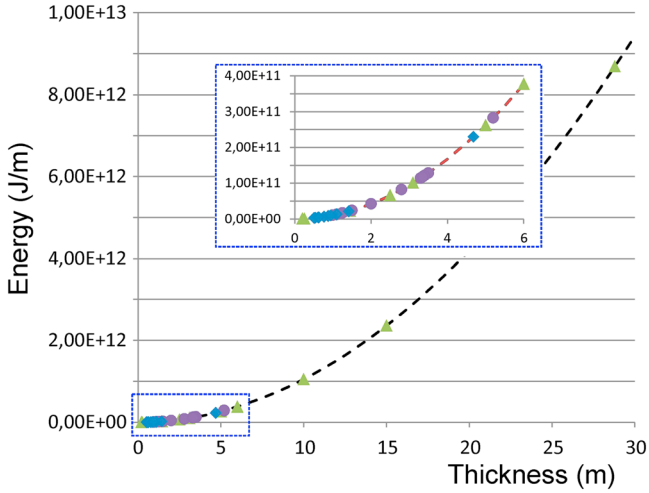

Figure 1. Expected available mechanical elastic plane strain energy U_E (J/m) that will be released during the dike propagation (dashed line) from equation (3). The energies expected for the modeled dikes of Japanese volcanoes (green triangles), Etna (purple circles), and Afar (blue rhombus) are shown. The modeled parameters of these volcanoes are reported in Table 1. The graph is calculated for a rigidity 10^{10} Pa and Poisson coefficient 0.25.

average thickness is often used in the equations relating overpressure and dike dimensions [e.g., *Gudmundsson*, 1983; *Geshi et al.*, 2010; *Geshi and Oikawa*, 2014]. In the following, we assume that dikes maintain an approximately constant thickness at any location during the entire propagation (only the early nucleation phase is excluded). This assumption, combined with equation (3) stating that the elastic strain energy depends on the squared thickness of the dike, implies that when a dike starts to propagate then from the determination of its opening, it may be possible to estimate the expected final energy to be released.

3. Seismic Energy and Application Case

Dike propagations are usually accompanied by seismic swarms tracking the migratory path of the intruding magma and mirroring the released energy. In quantifying the released energy, the seismic moment has the advantage of not only being the seismic energy which is radiated seismically, but it can be considered a measure of the total energy released during an earthquake. We considered several intrusions at different volcanoes: Etna (Italy), Izu, and Myiakejima (Japan), and the dikes from the 2005–2010 rifting episode at the Manda-Hararo rift segment in Afar (Ethiopia). We used available dike shape/dimensions modeled from ground deformation measurements and cumulative seismic moment of earthquakes recorded during propagation (Table 1). In Figure 1 we reported the available mechanical elastic strain energy that can be calculated from (3) varying the thickness according to the different dike cases, after fixing representative mean values of the elastic medium properties (rigidity and Poisson's ratio).

For each modeled dike, we multiplied U_E by the length of the dike in the direction perpendicular to the propagation (i.e., the estimated width reported in Table 1); thus, we obtain the total 3-D available mechanical elastic strain energy U_T. We compared U_T with the cumulative seismic moment M_o (Figure 2) and found the linear best fit law:

$$\log_{10}(M_o) = 1.41 \cdot \log_{10}(U_T) - 3.0 \tag{4}$$

with a correlation coefficient $R^2 = 0.63$ that reflects the spread of the data along the linear fit (Figure 2, top). The spread is mainly a consequence of the elastic parameters that we assumed equal ($\mu = 10^{10}$ Pa and $\nu = 0.25$) in the different volcano areas considered, and also of the different modeled thicknesses found for same intrusions such as the Izu 1998 and 2000 cases. Note also that without the outlier (Izu 1997 eruption) the fit improves considerably to $R^2 = 0.82$. The relation can be considered a first tool to estimate the expected seismic moment M_o from the available energy U_E that is calculated from (3) after the initial dike shape is known. If robust data for single volcano areas are available, then the fit quality can be improved and become more representative of the specific investigated volcano. In particular, for the recent eruptions of Etna volcano the modeled dike shapes and the seismic recordings are particularly robust thanks to both the integrated monitoring system of ground deformation (static and continuous GPS measurements and continuous borehole tilt) and the dense seismic network installed around the volcano. For this volcano the relationship (4) is particularly precise, becoming

$$\log_{10}(M_o) = 1.24 \cdot \log_{10}(U_T) - 1.54 \tag{5}$$

with a near same slope coefficient of the general case, confirming the validity of the relation, and a very good R^2 equal to 0.99 (Figure 2, bottom). In Figure 3 we report an application case regarding the October 2002

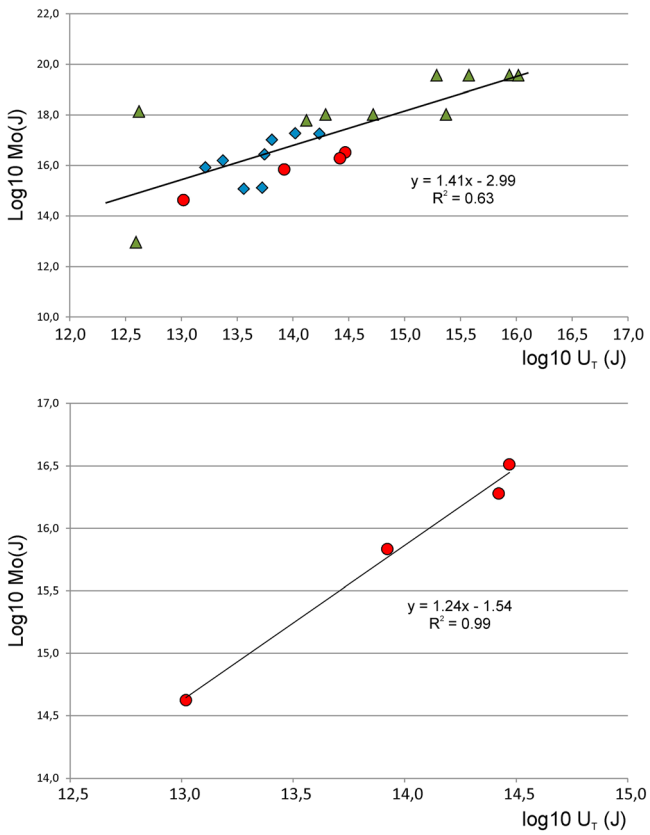

Figure 2. (top) Total seismic moment M_o (J) calculated from the seismicity recorded during the dike propagation versus total 3-D available mechanical elastic strain energy U_T (J) calculated from equation (3) for the different modeled dikes reported in Table 1. The linear law gives an empirical relation to translate the estimated energy U_T in expected cumulated seismic moment M_o. (bottom) Zoom of the data of Etna volcano having a much more precise fit.

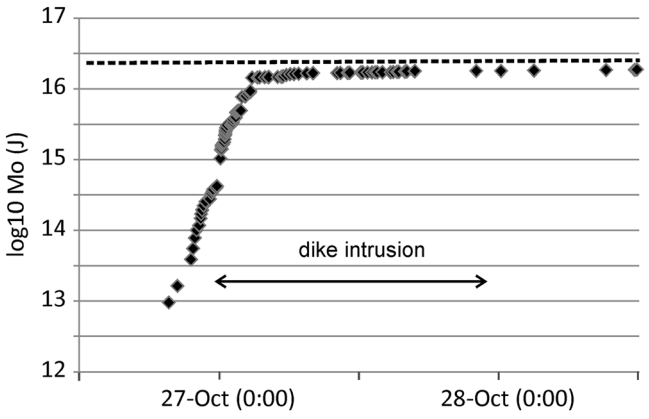

Figure 3. Applicative example of the October 2002 lateral intrusion in the NE flank of Etna. $Log_{10}(M_o)$ versus time. From the initial phases of the dike, after its opening is inferred, the available energy can be estimated from equation (3) and the expected total seismic moment to be released (dashed line) from equation (5). This M_o value is the limit to be reached by the cumulative recorded seismic moment to obtain the energy equilibrium and the dike stopping.

lateral intrusion in the NE flank of Etna volcano [*Aloisi et al.,* 2006, and references therein]. The dike propagated laterally northeastward in the NE flank during the whole day of 27 October, reaching a distance of nearly 5 km from the summit craters area. The main lava flow poured out from 2000 m above sea level (asl) where this lateral dike intersected the free surface.

On the surface it formed a line of several explosive cinder cones connected by a fissure from which lava flows were emitted. There was great concern that this eruptive fracture could have propagated further and discharged magma in a large flank eruption. This would have threatened the villages located on the mid-NE flank along the eruptive fissure direction. The temporal evolution of the dike was modeled by the continuously recorded borehole tiltmeters data [*Aloisi et al.,* 2006]. The reproduction of the recorded tilt signal allowed describing the geometry and characteristics of the propagating dike, inferring a near constant thickness of 3.35 m (Table 1). This modeled value was also confirmed by the field measurement of the dike in a segment exposed below the pit crater at 2200 m asl [*Branca et al.,* 2003]. Following our proposed approach, we can estimate the available elastic strain energy U_E and then from (5) we calculate the expected seismic moment M_o to be released. The recorded cumulated M_o approaches the expected limit of the cumulated M_o (Figure 3).

4. Discussion and Conclusive Remarks

The dike's uniform thickness can be considered a valid first-order assumption supported by different arguments and results. In fact, several worldwide volcano-tectonics studies assume constant thickness [e.g., *Delaney and Pollard*, 1981; *Marinoni*,

2000; *Klausen*, 2006] or use an average thickness [e.g., *Gudmundsson*, 1983]; statistical analysis of thousands of thickness data from different tectonic settings assume and use constant thickness for each single dike [e.g., *Krumbholz et al.,* 2014]. Structural geologists have used exposed dikes to relate their length and mean uniform thickness to the driving pressure generating them in order to infer constraints on the process of dike emplacement [e.g., *Delaney and Pollard*, 1981; *Reches and Fink*, 1988; *Delaney and Gartner*, 1997; *Valentine and Krogh*, 2006; *Poland et al.,* 2008].

In the field of mechanical elastic strain, the length of the dike is also related with the energy. However, we would highlight that its final extension cannot be estimated with precision at the beginning of the propagation. In fact, for a same quantity of energy to be released a dike may travel different lengths due to possible structural conditions (e.g., barriers) or stiffness variation that could cause its propagation to stop. But the interesting point we underline is that although under different conditions a dike could travel different lengths, the certain aspect is that the available mechanical elastic strain energy has to be entirely released and, as shown in our study, it can be a priori estimated by the dike opening. In other words, the thickness is the most unequivocal parameter related to the energy to be released.

Many authors have compared intrusive volumes and seismic energy released [*McGarr*, 2014; *White and McCausland*, 2016]. They found a linear relation between $\log_{10}$(Vol) and $\log_{10}(M_o)$ similarly to our linear relation between $\log_{10}(U_T)$ and $\log_{10}(M_o)$ presented in Figure 2. The approach is similar to ours because the volume correlates with the elastic energy used to open the dike. However, for a forecasting approach able to quantify the expected energy, this approach is limited by being dependent on the final length that as discussed above, cannot be evaluated a priori. Our thickness approach has the advantage of being based on the peculiarity that the energy expected can be estimated at the beginning of the intrusion through the estimation of the dike opening when its effect on the surface begins to be revealed by the deformation monitoring systems. This parameter can immediately be inferred as soon as the deformation monitoring systems (GPS, tilt, and strain) detect the first significant changes. The released energy can be related to seismic moment Mo that has the advantage of being calculable in near real time since it is related to the seismic local magnitude that is easily determined from the seismic recordings. The comparison of the seismic moment expected by the release of the available energy with the moment calculated in real time by observing networks provides a prediction of when the energy is balancing and hence when the dike is expected to stop. This helps answer one of the fundamental questions raised by civil protection authorities on lateral dike propagation, namely, "*how long will the eruptive fissure propagate?*" As shown in the application case reported in the previous section, this approach may also prove a very useful new tool to estimate the dike propagation hazard during the early phase of an eruptive intrusion.

Acknowledgments
A.B. is particularly indebted to the technical staff of Ground Deformation Group of INGV-OE who ensured the regular working of the tilt and GPS monitoring networks, which enabled the previous studies during the last three decades. A.B. has benefited from a short-term application visit to ERI-Tokyo University, where the study was initiated and preliminarily discussed among the authors. We thank an anonymous referee and, in particular, A. Gudmundsson for the constructive comments and suggestions that helped us to improve the manuscript clarity. We thank S. Conway for revising the English language of the manuscript. All data for this paper are properly cited and referred in the reference list reported in Table 1.

References

Acocella, V., M. Neri, and G. Norini (2013), An overview of experimental models to understand a complex volcanic instability: Application to Mount Etna, Italy, *J. Volcanol. Geotherm. Res.*, *251*, 98–111.

Aloisi, M., A. Bonaccorso, and S. Gambino (2006), Imaging composite dike propagation (Etna 2002, case), *J. Geophys. Res.*, *111*, B06404, doi:10.1029/2005JB003908.

Alparone, S., et al. (2015), Instrumental seismic catalogue of Mt. Etna earthquakes (Sicily, Italy): Ten years (2000-2010) of instrumental recordings, *Ann. Geophys.*, *58*, 4, doi:10.4401/ag-6591.

Aoki, Y., P. Segall, T. Kato, P. Cervelli, and S. Shimada (1999), Imaging magma transport during the 1997 seismic swarm off the Izu peninsula, Japan, *Science*, *286*(5441), 927–930, doi:10.1126/science.286.5441.927.

Bonaccorso, A. (1996), A dynamic inversion for modelling volcanic sources through ground deformation data (Etna 1991–92), *Geophys. Res. Lett.*, *23*(5), 451–454.

Bonaccorso, A. (1999), The March 1981 Mt. Etna eruption inferred through ground deformation modelling, *Phys. Earth Planet. Inter.*, *112*, 125–136.

Bonaccorso, A., and P. M. Davis (1993), Dislocation modelling of the 1989 dike intrusion into the flank of the Mt. Etna, Sicily, *J. Geophys. Res.*, *98*(3), 4261–4268.

Bonaccorso, A., M. Aloisi, and M. Mattia (2002), Dike emplacement forerunning the Etna July 2001 eruption modelled through continuous tilt and GPS data, *Geophys. Res. Lett.*, *29*(13), 2-1–2-4, doi:10.1029/2001GL014397.

Bonafede, M., and E. Rivalta (1999), The tensile dislocation problem in a layered elastic medium, *Geophys. J. Int.*, *136*(2), 341–356, doi:10.1046/j.1365-246X.1999.00645.x.

Branca, S., D. Carbone, and F. Greco (2003), Intrusive mechanism of the 2002 NE-rift eruption at Mt. Etna (Italy) inferred through continuous microgravity data and volcanological evidences, *Geophys. Res. Lett.*, *30*(20), 2077, doi:10.1029/2003GL018250.

Daniels, K. A., and T. Menand (2015), An experimental investigation of dyke injection under regional extensional stress, *J. Geophys. Res. Solid Earth*, *120*, 2014–2035, doi:10.1002/2014JB011627.

Delaney, P. T., and D. D. Pollard (1981), Deformation and host rocks and flow of magma during growth of Minette dikes and breccia-bearing intrusions near Shiprock, New Mexico, *U.S. Geol. Surv. Prof. Pap., 1202*, Washington.
Delaney, P. T., and A. E. Gartner (1997), Physical processes of shallow mafic dike emplacement near the San Rafael Swell, Utah, *Geol. Soc. Am. Bull.*, *109*, 1177–1192.
Del Negro, C., A. Cappello, G. Bilotta, G. Ganci, and A. Herault (2016), Risk from lava flow inundations in densely populated areas: The case of Etna volcano, Abstract V12A-08, presented at 2016 Fall Meeting, AGU, San Francisco, Calif., 12–16 Dec.
Ferrari, L., V. H. Garduno, and M. Neri (1991), I dicchi della Valle del Bove, Etna: Un metodo per stimare le dilatazioni di un apparato vulcanico [in Italian with English abstract], *Mem. Soc. Geol. It.*, *47*, 495–508.
Geshi, N., and T. Oikawa (2014), The spectrum of basaltic feeder systems from effusive lava eruption to explosive eruption at Miyakejima volcano, *Jpn. Bull. Volcanol.*, *76*, 797, doi:10.1007/s00445-014-0797-7.
Geshi, N., S. Kusumoto, and A. Gudmundsson (2010), Geometric difference between non-feeder and feeder dikes, *Geology*, *38*(3), 195–198, doi:10.1130/G30350.1.
Geshi, N., S. Kusumoto, and A. Gudmundsson (2012), Effects of mechanical layering of host rocks on dike growth and arrest, *J. Volcanol. Geotherm. Res.*, *223–224*, 74–82.
Giampiccolo, E., S. D'Amico, D. Patanè, and S. Gresta (2007), Attenuation and source parameters of shallow Microearthquakes at Mt. Etna volcano, Italy, *Bull. Seismol. Soc. Am.*, *97*(1B), 184–197, doi:10.1785/0120050252.
Grandin, R., A. Socquet, E. Jacques, N. Mazzoni, J. B. de Chebalier, and G. King (2010), Sequence of rifting in Afar, Manda-Hararo rift, Ethiopia, 2005–2009: Time–space evolution and interactions between dikes from interferometric synthetic aperture radar and static stress change modeling, *J. Geophys. Res.*, *115*, B10413, doi:10.1029/2009JB000815.
Grandin, R., E. Jacques, A. Nercessian, A. Ayele, C. Doubre, A. Socquet, D. Keir, M. Kassim, A. Lemarchand, and G. C. P. King (2011), Seismicity during lateral dike propagation: Insights from new data in the recent Manda Hararo–Dabbahu rifting episode (Afar, Ethiopia), *Geochem. Geophys. Geosyst.*, *12*, Q0AB08, doi:10.1029/2010GC003434.
Griffith, A. A. (1921), The phenomena of rupture and flow in solids, *Philos. Trans. R. Soc. London, Ser. A*, *221*, 163–198.
Gudmundsson, A. (1983), Form and dimensions of dykes in eastern Iceland, *Tectonophysics*, *95*, 295–307.
Gudmundsson, A. (2002), Emplacement and arrest of sheets and dykes in central volcanoes, *J. Volcanol. Geotherm. Res.*, *116*, 279–298.
Gudmundsson, A. (2003), Surface stresses associated with arrested dykes in rift zones, *Bull. Volcanol.*, *65*, 606–619.
Gudmundsson, A. (2006), How local stresses control magma-chamber ruptures, dyke injections, and eruptions in composite volcanoes, *Earth Sci. Rev.*, *79*, 1–31.
Gudmundsson, A. (2009), Toughness and failure of volcanic edifices, *Tectonophysics*, *471*, 27–35.
Gudmundsson, A. (2011), Deflection of dykes into sills at discontinuities and magma-chamber formation, *Tectonophysics*, *500*, 50–64.
Gudmundsson, A. (2016), The mechanics of large volcanic eruptions, *Earth Sci. Rev.*, *163*, 72–93.
Gudmundsson, A., L. B. Marinoni, and J. Martí (1999), Injection and arrest of dykes: Implications for volcanic hazards, *J. Volcanol. Geotherm. Res.*, *88*, 1–13, doi:10.1016/S0377-0273[98]00107-3.
Heimpel, M., and P. Olson (1994), in *Buoyancy-Driven Fracture and Magma Transport Through the Lithosphere: Models and Experiments*, edited by M. Ryan, pp. 223–240, Magmatic Systems, Academic Press, New York.
Hotta, K., M. Iguchi, and T. Tameguri (2016), Rapid dike intrusion into Sakurajima volcano on August 15, 2015, as detected by multi-parameter ground deformation observations, *Earth Planets Space*, *68*, 68, doi:10.1186/s40623-016-0450-0.
Ito, T., and S. Yoshioka (2002), A dike intrusion model in and around Miyakejima, Nijima and Kozushima in 2000, *Tectonophysics*, *569*, 171–187.
Irwin, G. R. (1957), Analysis of stresses and strains near the end of a crack traversing a plate, *J. Appl. Mech.*, *24*, 361–364.
Lister, J. R., and R. C. Kerr (1991), Fluid-mechanical models of crack propagation and their application to magma transport in dykes, *J. Geophys. Res.*, *96*, 10,049–10,077.
Kavanagh, J. L., and R. S. J. Sparks (2011), Insights of dyke emplacement mechanics from detailed 3D dyke thickness datasets, *J. Geol. Soc. London*, *168*, 965–978, doi:10.1144/0016-76492010-137.
Klausen, M. B. (2006), Similar dyke thickness variation across three volcanic rifts in the North Atlantic region: Implications for intrusion mechanisms, *Lithos*, *92*, 137–153.
Krumbholz, M., C. F. Hieronymus, S. Burchardt, V. R. Troll, D. C. Tanner, and N. Friese (2014), Weibull-distributed dyke thickness reflects probabilistic character of host-rock strength, *Nat. Commun.*, *5*, 3272, doi:10.1038/ncomms4272.
Ji, L., Z. Lu, D. Dzurisin, and S. Senyukov (2013), Pre-eruption deformation caused by dike intrusion beneath Kizimen volcano, Kamchatka, Russia, observed by InSAR, *J. Volcanol. Geotherm. Res.*, *256*, 87–95.
Maccaferri, F., E. Rivalta, L. Passarelli, and Y. Aoki (2015), On the mechanisms governing dike arrest: Insight from the 2000 Miyakejima dike injection, *Earth Planet. Sci. Lett.*, *434*(64–7), 42016, doi:10.1016/j.epsl.2015.11.024.
Marinoni, L. B. (2000), Crustal extension from exposed sheet intrusions: Review and method proposal, *J. Volcanol. Geotherm. Res.*, *107*(1–3), 27–46.
McGarr, A. (2014), Maximum magnitude earthquakes induced by fluid injection, *J. Geophys. Res. Solid Earth*, *119*, 1008–1019, doi:10.1002/2013JB010597.
McLeod, P., and S. Tait (1999), The growth of dykes from magma chambers, *J. Volcanol. Geotherm. Res.*, *92*(3–4), 231–245.
Menand, T., and S. Tait (2002), The propagation of a buoyant liquid-filled fissure from a source under constant pressure: An experimental approach, *J. Geophys. Res.*, *107*(B11), 2306, doi:10.1029/2001JB000589.
Morishita, Y., T. Kobayashi, and H. Yarai (2016), Three-dimensional deformation mapping of a dike intrusion event in Sakurajima in 2015 by exploiting the right- and left-looking ALOS-2 InSAR, *Geophys. Res. Lett.*, *43*, 4197–4204, doi:10.1002/2016GL068293.
Morita, Y., S. Nakao, and Y. Hayashi (2006), A quantitative approach to the dike intrusion process inferred from a joint analysis of geodetic and seismological data for the 1998 earthquake swarm off the east coast of Izu peninsula, central Japan, *J. Geophys. Res.*, *111*, B06208, doi:10.1029/2005JB003860.
Murray, J. B., and A. D. Pullen (1984), Three dimensional model of the feeder conduit of the 1983 eruption of Mt. Etna volcano from ground deformation measurements, *Bull. Volcanol.*, *47*(4), 1145–1163.
Napoli, R., G. Currenti, C. Del Negro, F. Greco, and D. Scandura (2008), Volcanomagnetic evidence of the magmatic intrusion on 13th May 2008 Etna eruption, *Geophys. Res. Lett.*, *35*, L22301, doi:10.1029/2008GL035350.
Okada, Y., and E. Yamamoto (1991), Dike intrusion model for the 1989 seismovolcanic activity off Ito, central Japan, *J. Geophys. Res.*, *96*, 10,361–10,376.
Ozawa, S., S. Miyazaki, T. Nishimura, M. Murakami, M. Kaidzu, T. Imakiire, and X. Ji (2004), Creep, dike intrusion, and magma chamber deflation model for the 2000 Miyake eruption and the Izu Islands earthquakes, *J. Geophys. Res.*, *109*, B02410, doi:10.1029/2003JB002601.

Peltier, A., V. Ferrazzini, T. Staudacher, and P. Bachèlery (2005), Imaging the dynamics of dyke propagation prior to the 2000–2003 flank eruptions at Piton de la Fourniase, Reunion Island, *Geophys. Res. Lett.*, *32*, L22302, doi:10.1029/2005GL023720.

Poland, M. P., W. P. Moats, and J. H. Fink (2008), A model for radial dike emplacement in composite cones based on observations from Summer Coon volcano, Colorado, USA, *Bull. Volcanol.*, *70*, 861–875, doi:10.1007/s00445-007-0175-9.

Pollard, D. D. (1987), Elementary fracture mechanics applied to the structural interpretation of dykes, in *Mafic Dyke Swarms*, *Geol. Assoc. Canada*, vol. 34, edited by H. C. Halls, and W. H. Fahrig, pp. 112–128.

Pollard, D. D., and O. H. Muller (1976), The effect of gradients in regional stress and magma pressure on the Form of sheet intrusions in cross section, *J. Geophys. Res.*, *81*, 5.

Reches, Z., and J. Fink (1988), The mechanism of intrusion of the Inyo Dike, Long Valley aldera, California, *J. Geophys. Res.*, *93*, 4321–4334.

Rivalta, E. (2010), Evidence that coupling to magma chambers controls the volume history and velocity of laterally propagating intrusions, *J. Geophys. Res.*, *115*, B07203, doi:10.1029/2009JB006922.

Rivalta, E., B. Taisne, A. P. Bunger, and R. F. Katz (2015), A review of mechanical models of dike propagation: Schools of thought, results and future directions, *Tectonophysics*, *638*, 1–42.

Rubin, A. M. (1990), A comparison of rift-zone tectonics in Iceland and Hawaii, *Bull. Volcanol.*, *52*, 302–319.

Rubin, A. M. (1993), Tensile fracture of rock at high confining pressure: Implications for dike propagation, *J. Geophys. Res.*, *98*, 15919–15935.

Rubin, A. (1995), Propagation of magma-filled cracks, *Annu. Rev. Earth Planet. Sci.*, *23*, 287–336.

Rubin, A. M., and D. D. Pollard (1987), Origins of blade-like dikes in volcanic rift zones, in *Volcanism in Hawaii*, *U.S. Geol. Surv. Prof. Pap., 1350*, edited by R. D. Decker, T. L. Wright, and P. H. Stauffer, pp. 1449–1470.

Rubin, A. M., and D. D. Pollard (1988), Dike-induced faulting in rift zones of Iceland and Afar, *Geology*, *16*, 413–417.

Rubin, A. M., D. Gillard, and A. Got (1998), Reinterpretation of seismicity associated with the January 1983 dike intrusion at Kilauea Volcano, Hawaii, *J. Geophys. Res.*, *103*, 10,003–10,015.

Segall, P., P. Cervelli, S. Owen, M. Lisowski, and A. Miklius (2001), Constraints on dike propagation from continuous GPS measurements, *J. Geophys. Res.*, *106*, 19,301–19,317.

Sigmundsson, F., et al. (2015), Segmented lateral dyke growth in a rifting event at Bardarbunga volcanic system, Iceland, *Nature*, *517*, 191–195.

Takada, A. (1990), Experimental study on propagation of liquid-filled crack in gelatin: Shape and velocity in hydrostatic stress condition, *J. Geophys. Res.*, *95*, 8471–8481.

Taisne, B., and S. Tait (2009), Eruption versus intrusion? Arrest of propagation of constant volume, buoyant, liquid-filled cracks in an elastic, brittle host, *J. Geophys. Res.*, *114*, B06202, doi:10.1029/2009JB006297.

Taisne, B., S. Tait, and C. Jaupart (2011), Conditions for the arrest of a vertical propagating dyke, *Bull. Volcanol.*, *73*, 191–204.

Traversa, P., V. Pinel, and J. R. Grasso (2010), A constant influx model for dike propagation: Implications for magma reservoir dynamics, *J. Geophys. Res.*, *115*, B01201, doi:10.1029/2009JB006559.

Valentine, G. A., and K. E. C. Krogh (2006), Emplacement of shallow dikes and sills beneath a small basaltic volcanic center—The role of pre-existing structure [Paiute Ridge, southern Nevada, USA], *Earth Planet. Sci. Lett.*, *246*, 217–230.

Yamaoka, K, M. Kawamura, F. Kimata, N. Fujii, and T. Kudo (2005), Dike intrusion associated with the 2000 eruption of Miyakejima Volcano, Japan, *Bull. Volcanol.*, *67*, 231–242, doi:10.1007/s00445-004-0406-2.

White, R., and W. McCausland (2016), Volcano-tectonic earthquakes: A new tool for estimating intrusive volumes and forecasting eruptions, *J. Volcanol. Geotherm. Res.*, *309*, 139–155.

Xu, W., S. Jónsson, F. Corbi, and E. Rivalta (2016), Graben formation and dikearrest during the 2009 Harrat Lunayyir dike intrusion in Saudi Arabia: Insights from InSAR, stress calculations and analog experiments, *J. Geophys. Res. Solid Earth*, *121*, 2837–2851, doi:10.1002/2015JB012505.